Supporting Information for:
Tuning the Dzyaloshinskii−Moriya Interaction in Pt/Co/MgO heterostructures through MgO thickness

Anni Cao,[a, 1)] Xueying Zhang,[ab, 1)] Bert Koopmans,[c] Shouzhong Peng,[a] Yu Zhang,[ab] Zilu Wang,[a] Shaohua Yan,[a] Hongxin Yang,[d] and Weisheng Zhao*[a]

* Corresponding authors

[a] Fert Beijing Institute, BDBC, School of Electronic and Information Engineering, Beihang University, Beijing, China

[b] Centre for Nanoscience and Nanotechnology, University Paris-Saclay, Orsay, France

[c] Department of Applied Physics, Institute for Photonic Integration, Eindhoven University of Technology, Eindhoven, The Netherlands

[d] Key Laboratory of Magnetic Materials and Devices, Ningbo Institute of Materials Technology and Engineering, Chinese Academy of Sciences, Ningbo, Zhejiang, China

I. Exponentially-varied v versus $H_z^{-\frac{1}{4}}$

The determination of DMI by the asymmetry of DW velocity is based on the creep mode DW motion. We measured the DW velocity v with different driven field value H_z to improve the feasibility of the measurement, according to the characterization of the creep mode motion which could be described as

$$v \sim exp\left(-\alpha H_z^{-\frac{1}{4}}\right) \quad \text{(S1).}$$

The results of samples without and with Mg insertion layer were shown below. All the driven fields we use to measure the H_{DMI} circled by red-dotted line are inside the linear regions in Figure S1 S2.

1) Anni Cao and Xueying Zhang contributed equally to this work.

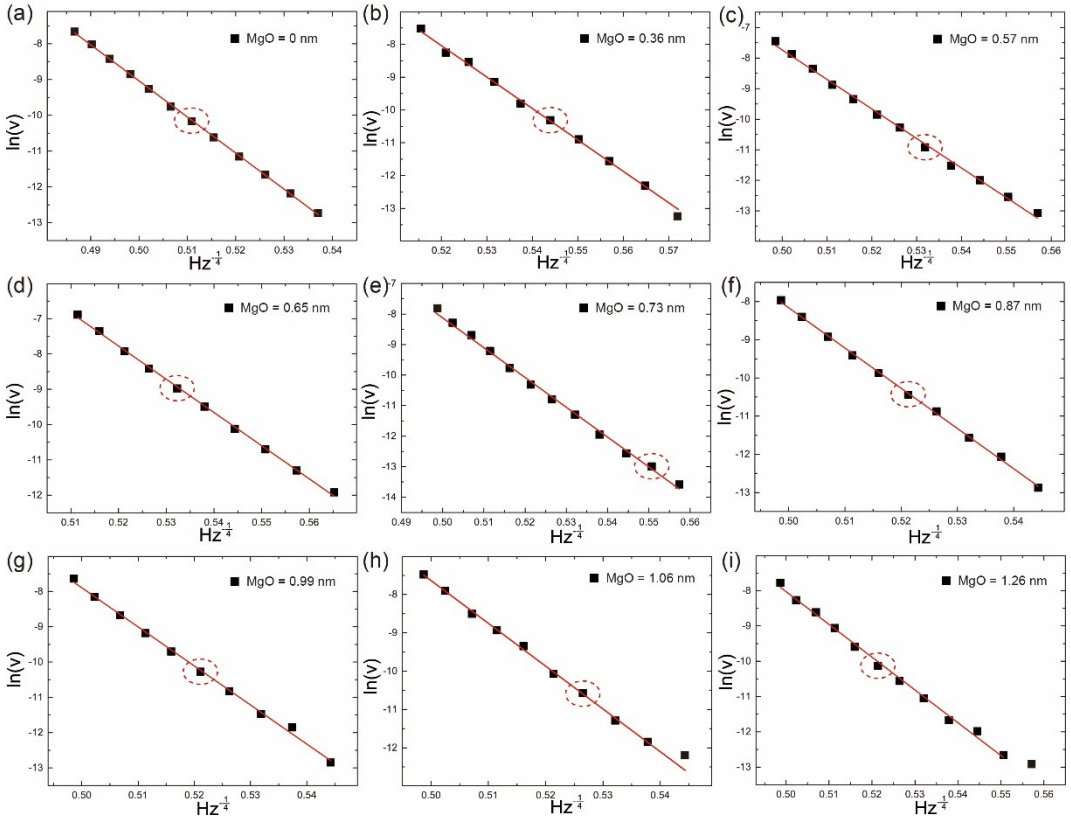

Figure S1. Fitting lines of $H_z^{-\frac{1}{4}} - ln[r0](v)$ for samples with different MgO thickness when there is no Mg inserted.

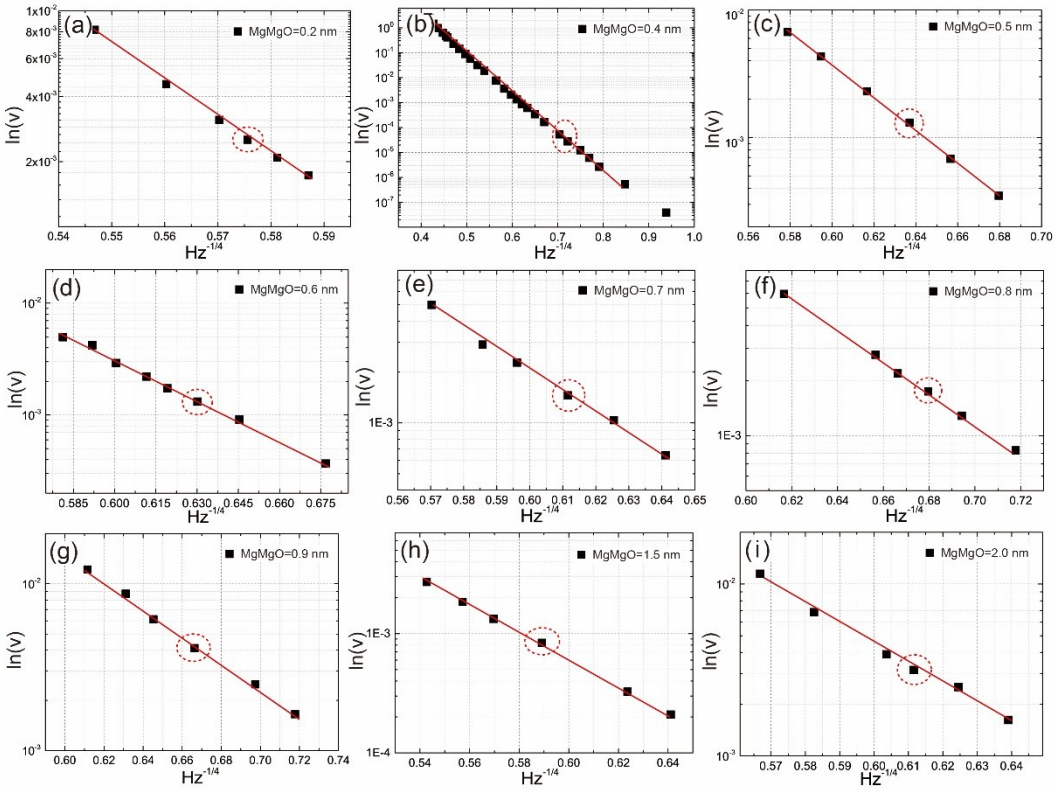

Figure S2. Fitting lines of $H_z^{-\frac{1}{4}} - ln[r0](v)$ for samples with different MgO thickness when there is 0.2 nm Mg inserted.

II. H_{DMI} with different H_z

In order to prove that the driven field H_z has no effect on the effective DMI field H_{DMI}, the equi-speed contour maps of $t_{MgO} = 0.40, 0.52\ and\ 0.77\ nm$ samples with 1.00 nm Co layer were shown in the Figure S6.

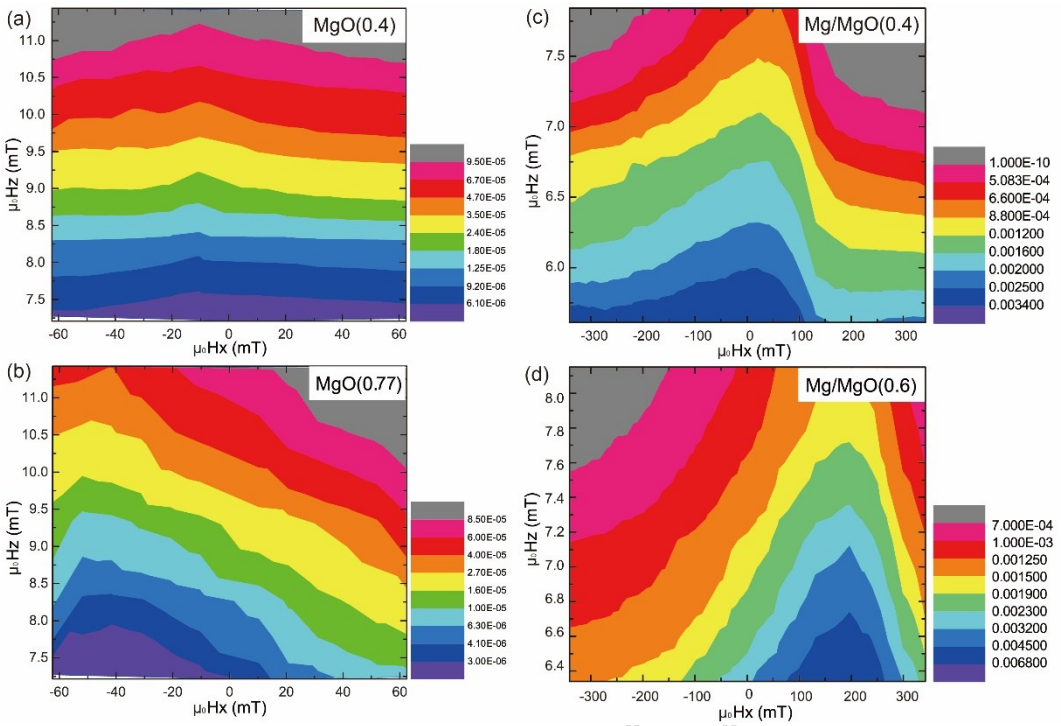

Figure S3. Two-dimensional equi-speed contour map of v as a function of $\mu_0 H_x$ and $\mu_0 H_z$. The color corresponds to the magnitude of v with the scale on the right.

III. Calculation of the demagnetizing field and the stray field

Using the concept of magnetization current[1,2], we numerically calculated the demagnetizing field as shown in Figure S7 (a), magnetic domains can be infinitely divided into small magnetic elements. Each element is equivalent to a ring current element, with current per unit area $I = t * M_S$, where t is the thickness of magnetic layer and M_S is the saturated magnetization per volume. For a uniformly magnetized out-of-plane domain, the current of one magnetic element can always be cancelled out by the current of the neighboring ones, except for elements in the boundary of domains and the edge of the sample. Namely, the magnetization currents are zero inside or outside the domain. The only non-zero contributions are on the boundary of the domain and the edge of the sample which are together noted as demagnetizing field here.

The contribution of the domain boundary is equal to the Oersted field produced by the effective current at the edge of domains. For a magnetic bubble with radius r in a magnetic thin film, the electrical circuit is plotted in Figure S4 (b). In addition, the DW width in PMA samples[3] could be estimated as 10 nm, and we have testified the width wouldn't strongly influence the demagnetizing field. This width is considered as the distance between two domains with opposite

magnetization, i.e. the distance between the two circular current circuits. Similarly, the contribution of the sample edge is closely related to the distance d between DWs and the edge of sample, as showed in Figure S4 (b).

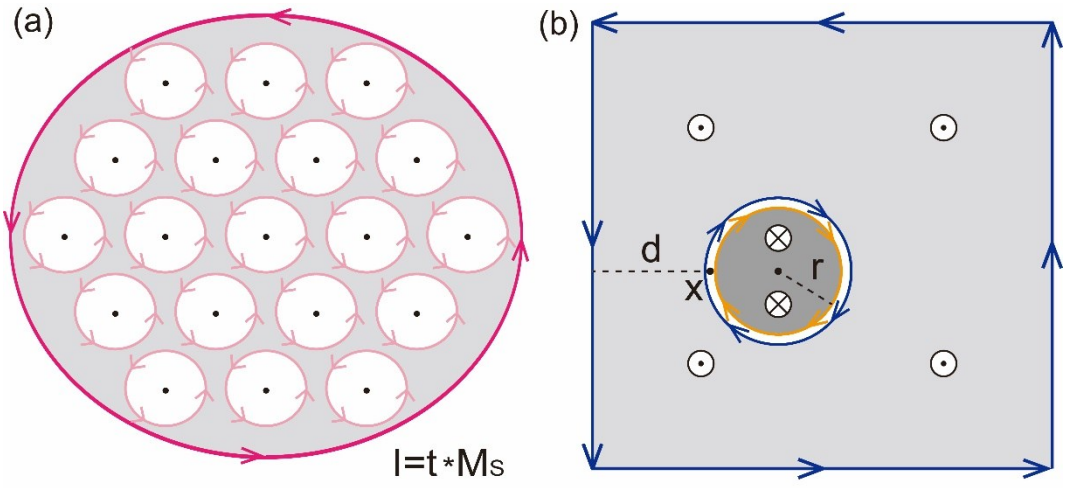

Figure S4. Magnetization current of the magnetic structure. (a) Sketch to show the concept of magnetization current. (b) Electrical circuit identical to the current created by the magnetization at the edges of the structure and along the DW. Then, the stray field can be calculated using the Biot-Savart's law.

Using MATLAB, we respectively calculated the demagnetizing field $\mu_0 H_{de} = \mu_0 H_{DW} + \mu_0 H_{sample}$ at point X shown in Figure S4, with r varying from 100 μm to 250 μm (the size range of DW we observed) and d varying from 120 μm (the minimum distance of our photo results) to 5×10^6 μm (the measured sample size). The results are plotted in Figure S5. It can be seen that, with the growth of bubble domains the demagnetizing field $\mu_0 H_{de}$ is lower than 0.023 mT, and as the distance to sample edge increases, the variation of $\mu_0 H_{de}$ is always less than 0.002 mT which can be neglected.

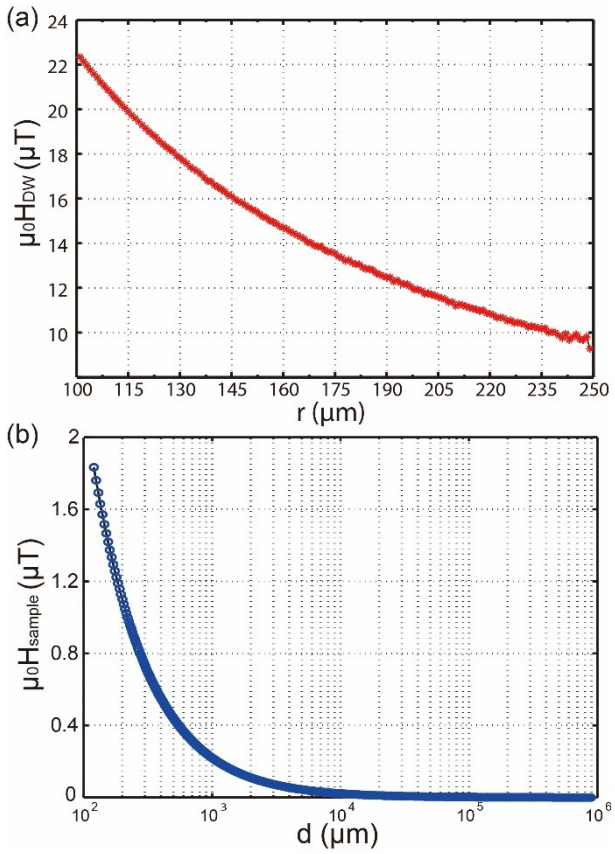

Figure S5. Numerically calculated demagnetizing field at point P as a function of the inverse of bubble radius, (a) the Oersted field of the effective current at the boundary of the observed DW $\mu_0 H_{DW}$, (b) the Oersted field of the effective current at the sample edge $\mu_0 H_{sample}$.

REFERENCES

1 E. Purcell, *Electricity and Magnetism*, 1963.

2 N. Vernier, J. P. Adam, S. Eimer, G. Agnus, T. Devolder, T. Hauet, B. Ocker, F. Garcia and D. Ravelosona, *Appl. Phys. Lett.*, 2014, **104**, 122404.

3 C. Burrowes, N. Vernier, J. P. Adam, L. Herrera Diez, K. Garcia, I. Barisic, G. Agnus, S. Eimer, J. Von Kim, T. Devolder, A. Lamperti, R. Mantovan, B. Ockert, E. E. Fullerton and D. Ravelosona, *Appl. Phys. Lett.*, 2013, **103**, 182401.